



Kinetic control of stationary flux ratios for a wide range of biochemical processes

Joel D. Mallory^a, Anatoly B. Kolomeisky^{a,b,c,d,1,2}, and Oleg A. Igoshin^{a,b,e,1,2}

^aCenter for Theoretical Biological Physics, Rice University, Houston, TX 77005; ^bDepartment of Chemistry, Rice University, Houston, TX 77005; ^cDepartment of Chemical and Biomolecular Engineering, Rice University, Houston, TX 77005; ^dDepartment of Physics and Astronomy, Rice University, Houston, TX 77005; and ^eDepartment of Bioengineering and of Biosciences, Rice University, Houston, TX 77005

Edited by James T. Hynes, University of Colorado Boulder, Boulder, CO, and approved March 10, 2020 (received for review November 28, 2019)

One of the most intriguing features of biological systems is their ability to regulate the steady-state fluxes of the underlying biochemical reactions; however, the regulatory mechanisms and their physicochemical properties are not fully understood. Fundamentally, flux regulation can be explained with a chemical kinetic formalism describing the transitions between discrete states, with the reaction rates defined by an underlying free energy landscape. Which features of the energy landscape affect the flux distribution? Here we prove that the ratios of the steady-state fluxes of quasi-first-order biochemical processes are invariant to energy perturbations of the discrete states and are only affected by the energy barriers. In other words, the nonequilibrium flux distribution is under kinetic and not thermodynamic control. We illustrate the generality of this result for three biological processes. For the network describing protein folding along competing pathways, the probabilities of proceeding via these pathways are shown to be invariant to the stability of the intermediates or to the presence of additional misfolded states. For the network describing protein synthesis, the error rate and the energy expenditure per peptide bond is proven to be independent of the stability of the intermediate states. For molecular motors such as myosin-V, the ratio of forward to backward steps and the number of adenosine 5'-triphosphate (ATP) molecules hydrolyzed per step is demonstrated to be invariant to energy perturbations of the intermediate states. These findings place important constraints on the ability of mutations and drug perturbations to affect the steady-state flux distribution for a wide class of biological processes.

properties of biological processes | nonequilibrium stationary dynamics | kinetic control | chemical kinetic analysis

Chemical kinetics represents a fundamental mesoscopic formalism to understand many biological phenomena with a wide range of major cellular processes described in terms of the complex networks of biochemical reactions (1). When the mechanistic details of the process are known, the underlying mechanisms can be represented as elementary steps described by mass-action kinetics of first-order reactions (e.g., for catalysis, conformational transitions, and dissociation) or second-order reactions for bimolecular binding transitions. This formalism allows one to study the kinetics of enzymatically controlled reactions and resulting kinetic laws (2), transformations between different states of promoters and resulting transcription rates (3–6), transitions between receptor complexes and resulting signaling (7, 8), and many other phenomena (9, 10). In many of these examples, the timescale of changes in the concentrations of unbound molecular species is much slower than the timescale of transitions between the states of the macromolecular systems. For example, concentrations of substrates and products of enzymatic catalysis change much more slowly than transitions between the different enzyme states (11). In this regime, second-order binding reactions can be effectively approximated as quasi-first-order transitions. As a result, the kinetic equations are linear, yielding a so-called linear framework (12). In

the steady state, the resulting linear algebraic equations can be easily solved to compute probabilities, fluxes, and many other important quantities.

For an arbitrary chemical network with elementary chemical transitions, the kinetics can be fundamentally understood in terms of the underlying free energy landscape. Assuming that thermal equilibrium in each chemical state is reached much faster than the timescale of the chemical transitions, the rate of each step can be expressed in terms of the activation energy, that is, the difference between the energy of the state and the barrier separating the states (13). The resulting expression of the rate constants is often referred to as the transition state theory (14). We note that, in this picture, the free energy landscape emerges naturally as a consequence of the microscopic description of a process through elementary chemical steps.

For reaction networks with cycles that do not change the concentrations of the molecular species in the cellular environment, the underlying chemical reaction rates are subject to the detailed balance constraints (15). In that case, the resulting steady-state probabilities are computed from the Boltzmann distribution, and they only depend on the free energy of the states that are independent of the free energy barriers (15). For example, models of binding and dissociation of transcription factors to DNA and resulting transcription rates in bacteria

Significance

Chemical kinetic formalism is widely used to describe biochemical processes, including channel transport, enzymatic catalysis, genetic regulation, and signal transduction. Fundamentally, transitions between biochemical states are defined by the underlying free energy landscapes, but few general results relate the landscape features to biologically relevant properties. At equilibrium, the probabilities of discrete states only depend on their energies and not on the energy barriers in between states. However, few general claims about nonequilibrium steady states have been formulated. Here, for nonequilibrium steady states of networks with quasi-order transitions, we prove that the flux ratios are invariant to energy perturbations of the states and, therefore, are only affected by the free energy barriers. Biological implications of the result are illustrated for three distinct biological processes.

Author contributions: A.B.K. and O.A.I. designed research; J.D.M., A.B.K., and O.A.I. performed research; J.D.M. analyzed data; and J.D.M., A.B.K., and O.A.I. wrote the paper.

The authors declare no competing interest.

This article is a PNAS Direct Submission.

Published under the PNAS license.

¹A.B.K. and O.A.I. contributed equally to this work.

²To whom correspondence may be addressed. Email: igoshin@rice.edu or tolya@rice.edu.

This article contains supporting information online at <https://www.pnas.org/lookup/suppl/doi:10.1073/pnas.1920873117/-DCSupplemental>.

First published April 7, 2020.

are often calculated in the equilibrium thermodynamics framework (16, 17). This regime is often referred to as thermodynamic control, in contrast to the kinetic control regime when the barrier heights determine the resulting distributions (18). In many other biologically relevant cases, transitions between states of the macromolecular system are coupled with the changes in the pool of cellular cofactor molecules. If the cycles in the network change the chemical composition of the cellular environment, the system reaches a nonequilibrium steady state where nonvanishing net fluxes are possible (15). For example, transitions between states of enzymes and molecular motors can be coupled to the hydrolysis of adenosine 5'-triphosphate (ATP) (19, 20). In the nonequilibrium steady state, the steady-state probabilities and the fluxes can depend on the energies of the transition states. Thus, nonequilibrium steady states may be under a combination of thermodynamic and kinetic controls, and it is not clear which features of the free energy landscape control key system properties (21).

The nonzero values of net fluxes in the nonequilibrium steady state have important biological implications. For example, the rate of an enzymatic reaction, the speed of a molecular motor, and many other crucial characteristics are proportional to these steady-state fluxes (15, 22). Moreover, many important properties can be related to the ratios of the steady-state fluxes. Specifically, the enzyme selectivity or the error rate that quantifies the ability of enzymes to discriminate between right (cognate) and wrong (noncognate) substrates can be expressed as the ratio of the catalytic fluxes to the corresponding states (19, 21, 23). In the same way, the efficiency of a molecular motor can be expressed in terms of the ratio of forward-stepping and futile cycle fluxes (22, 24). Notably, our previous research (25) has shown that, for both Michaelis–Menten and the Hopfield kinetic proofreading (KPR) mechanism (19), the error rate is purely under kinetic control. As such, the error rate is only a function of the differences in the free energy barriers for pathways leading to the right and wrong substrates, and it is independent of the differences of the stabilities of the corresponding states. However, the results in ref. 25 were limited in scope and had no clear physical explanation. The generalization of these conclusions to the other quantities is not obvious.

In this work, we use a chemical kinetic formalism to determine how steady-state probabilities and the flux distribution of the underlying biochemical reactions are affected by perturbations of the underlying free energy landscape. We illustrate the generality and the biological implications of our results by specifically studying three diverse biological systems. The examples include 1) two alternative pathways for protein folding in the presence of misfolded error states, which is motivated by folding pathways in hen egg-white lysozyme (26, 27); 2) a Hopfield KPR network describing aminoacyl transfer RNA (aa-tRNA) selection during protein translation in the *Escherichia coli* ribosome (19, 25, 28–31); and 3) the myosin-V motor protein that walks along actin cytoskeleton filaments (22, 24).

The results demonstrate that an arbitrary ratio of the steady-state fluxes is invariant to the energy perturbations of the stabilities of the discrete states and, therefore, is only dependent on the free energy barriers. In other words, we demonstrate that the biological properties that are expressed in terms of the steady-state flux ratios are governed by kinetic and not by thermodynamic factors. These results have wide-ranging implications for the types of genetic or chemical perturbations capable of changing the steady-state flux distribution through biochemical reaction networks. Generally, the values of the free energy barriers correlate with the free energies of the states (32). However, even though mutations can perturb both the free energy barriers and the stability of the minima, it is important to know that the latter energy parameters do not affect the flux ratios. Thus, our result can

direct experimental measurements of the underlying free energy landscape.

Methods

Notation and Setup. Consider an arbitrary biochemical system described by the linear formalism (12), that is, by a chemical kinetic network with quasi-first-order transitions between N biochemical states (Fig. 1A) with the rate constant for a reaction $i \rightarrow j$ (i.e., a transition from the i th state to the j th state) denoted as k_{ij} . Generally, there could be multiple elementary reactions between states i and j . Therefore,

$$k_{ij} = \sum_{\omega} k_{ij}^{\omega}, \quad [1]$$

where the index ω runs over all of the possible reaction pathways $i \rightarrow j$. For each elementary reaction, the rate constants k_{ij}^{ω} can be expressed as the product of a prefactor and an exponential free energy barrier term (e.g., as in transition state theory),

$$k_{ij}^{\omega} = k_{ij}^{0\omega} e^{\epsilon_i - \epsilon_{ij}^{\dagger\omega}}, \quad [2]$$

in which the prefactors of the bimolecular reactions that were initially second order (i.e., with cofactor binding steps) included the dependence on the chemical potentials μ_{γ} of these cofactors (see *SI Appendix* for definition of the prefactor $k_{ij}^{0\omega} \neq k_{ji}^{0\omega}$). Here, ϵ_i is the energy of the i th state, and $\epsilon_{ij}^{\dagger\omega} = \epsilon_{j,i}^{\dagger\omega}$ are the transition state energies in units of $k_B T$ (Fig. 1B).

In the limit of $t \rightarrow \infty$, the system is characterized by a stationary probability distribution vector with N components, $\mathbf{P} = [P_1, P_2, \dots, P_N]^T$, that can be obtained by solving a set of steady-state equations subject to the normalization condition,

$$\mathbf{K} \cdot \mathbf{P} = \mathbf{0} \text{ and } \mathbf{1}^T \cdot \mathbf{P} = 1, \quad [3]$$

where $\mathbf{1}$ is an $N \times 1$ unit vector, and \mathbf{K} is an $N \times N$ rate matrix,

$$K_{j,i} = \begin{cases} k_{ij}, & \text{for } j \neq i \\ -\sum_{i \neq j} k_{ij}, & \text{for } j = i. \end{cases} \quad [4]$$

Assuming this matrix is not rank deficient, Eq. 3 has a unique solution for \mathbf{P} . The corresponding steady-state fluxes for $i \rightarrow j$ are given by $J_{ij}^{\omega} = k_{ij}^{\omega} P_i$.

Depending on whether the rate constants k_{ij}^{ω} are subject to the detailed balance constraints, this formalism can describe both equilibrium and nonequilibrium steady states. In the former case, the fluxes balance $J_{ij}^{\omega} = J_{ji}^{\omega}$, and the stationary probability distribution corresponds to the Boltzmann distribution (15). Below, we explore nonequilibrium steady-state fluxes and the probabilities.

Perturbation of the Free Energy Landscape. Consider a perturbation that decreases the energy of an arbitrary state m on the free energy landscape of the system by an amount $\Delta\epsilon_m$, that is, such that its energy changes to

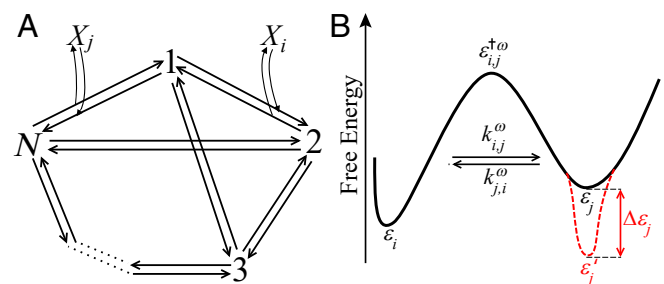


Fig. 1. General biochemical kinetic network and its free energy landscape. (A) Biochemical network comprising N different states. The discrete states are denoted by numbers $1, \dots, N$, and the cofactor molecules in the bath are denoted as X_i and X_j . (B) Free energy landscape for a reaction between states i and j with well depths ϵ_i and ϵ_j and the transition state energy $\epsilon_{ij}^{\dagger\omega}$. The rate constants k_{ij}^{ω} and k_{ji}^{ω} correspond to the forward and reverse reactions between the two states i and j on the pathway ω . Note that the energy of state j is decreased by an amount $\Delta\epsilon_j$ (red dashed curve) such that its energy is $\epsilon'_j = \epsilon_j - \Delta\epsilon_j$.

$\epsilon'_m = \epsilon_m - \Delta\epsilon_m$ (Fig. 1B). Here and below, the prime symbol \prime denotes the parameters following this perturbation. Assume that the energies of other states, namely, the transition state energies $\epsilon_{ij}^{\dagger\omega}$, and the chemical potentials μ_γ (SI Appendix, Eqs. S7–S9) of all of the cofactor molecules are held constant.

From Eq. 2, the perturbation reduces all of the rate constants for the reactions $m \rightarrow j$ by a factor of $e^{-\Delta\epsilon_m}$, but all of the other rate constants k_{ij}^ω remain the same. As a result, the perturbed steady-state probability distribution P' satisfies equations of the form of Eq. 3 with the perturbed matrix K' ,

$$K'_{j,i} = \begin{cases} K_{j,i}, & \text{for } i \neq m \\ K_{j,m}e^{-\Delta\epsilon_m}, & \text{for } i = m, \end{cases} \quad [5]$$

that is, with the entire m th column scaled by a factor of $e^{-\Delta\epsilon_m}$. It is not hard to show (SI Appendix, Eq. S19) that the perturbed probabilities P'_i can be expressed in terms of the unperturbed probabilities P_i as follows:

$$P'_i = \begin{cases} \alpha P_i, & \text{for } i \neq m \\ \alpha P_m e^{\Delta\epsilon_m}, & \text{for } i = m, \end{cases} \quad [6]$$

with normalization constant $\alpha = 1/(\sum_{j \neq m} P_j + P_m e^{\Delta\epsilon_m})$ that guarantees the conservation of probability, $\mathbf{1}^T \cdot \mathbf{P}' = 1$.

Invariance of the Ratios of the Steady-State Fluxes. From Eq. 6, we conclude that all of the steady-state fluxes are scaled by the same factor,

$$J'_{ij}{}^\omega \equiv k'_{ij}{}^\omega P'_i = \alpha J_{ij}{}^\omega, \quad \forall i \text{ and } j. \quad [7]$$

The factor α cancels out for all of the ratios of the perturbed steady-state fluxes, and we demonstrated that

$$\frac{\partial (J'_{ij}{}^\omega / J'_{ln}{}^\omega)}{\partial \Delta\epsilon_m} = 0, \quad \forall i (l) \text{ and } j (n). \quad [8]$$

Therefore, we conclude that the ratios of stationary fluxes or any of their linear combinations do not depend on the energies of the individual states ϵ_i and only depend on barrier heights ϵ_{ij}^\dagger .

Illustrative Examples. To illustrate the implications of Eq. 8, we use three major biological processes: protein folding networks inspired by hen egg-white lysozyme, a KPR network for aa-tRNA selection during protein translation in the *E. coli* ribosome, and the myosin-V motor protein that walks on the actin cytoskeleton filaments. For simplicity of the notation, we drop all of the prime \prime and ω superscripts on the perturbed steady-state fluxes.

Data Availability

The kinetic parameters used for illustrative examples from refs. 24, 27, 30–34 are given in SI Appendix, Tables S1–S3.

Results

Protein Folding Network. Protein folding is a fundamental process that is required for all living cells to maintain their proper functionality. Indeed, misfolded proteins and their aggregation have been linked to many types of pathological diseases (35). Protein folding occurs via a series of different funnels on a free energy landscape, and, as such, the process can be described using the chemical kinetic formalism for biochemical networks (15, 26, 27). Protein folding often does not require any energy consumption, and, therefore, it can be studied within the equilibrium thermodynamics framework (15, 35). On the other hand, in live cells, all proteins are synthesized in the unfolded states and degraded/diluted in the relatively stable folded states. In this situation, a nonequilibrium steady-state distribution of fluxes in a protein folding network can give information about the relative importance of different folding pathways and the probability of reaching incorrect metastable folding states.

Here, we consider a kinetic scheme representing the protein folding inspired by hen egg-white lysozyme (27, 33). For this enzyme, two mechanistic descriptions, namely, independent unrelated pathways (IUP) and predetermined pathways with optional error (PPOE), have been proposed. The IUP model (alias a heterogeneous folding) assumes that protein folding occurs through various intermediate states on different pathways that have no relationship to one another (26). On the other hand, the PPOE model supposes that all proteins fold cooperatively through the same productive pathway via partially folded subunits called foldons that resemble the correctly folded structure. However, during the folding process, the protein may also become diverted into multiple misfolded error states that hinder productive folding (26).

We chose a kinetic scheme (Fig. 2A) that combines the physicochemical aspects of both the IUP and PPOE models. There are two possible pathways for the unfolded protein in state 1 to reach the folded (native) conformation in state 3 on this biochemical kinetic network. This means that productive protein folding can proceed independently through either of the intermediate states 2 or 4. However, the protein may also become trapped in the misfolded error states denoted, respectively, as 5 and 6 on the two folding pathways. The misfolded error states 5 and 6 can be viewed as traps on the free energy landscape that might kinetically block productive protein folding into the folded conformation (state 3) on the two different pathways. To realize the nonequilibrium steady state and the nonzero fluxes in this network, we assume that the protein is synthesized in state 1 and degraded from state 3 with the rate constant $k_{\emptyset,1}$. In the nonequilibrium steady state, the synthesis and degradation fluxes are balanced so that we can map this scheme to the formalism considered in *Methods* by effectively introducing an irreversible $3 \rightarrow 1$ transition with the rate $k_{\emptyset,1}$ (similar to ref. 36).

We can now apply our analysis to ask how the steady-state folding flux splits between the top pathway via state 2 ($J_T = k_{1,2}P_1 - k_{2,1}P_2$) and the bottom pathway via state 4 ($J_B = k_{1,4}P_1 - k_{4,1}P_4$). Eq. 8 implies that the steady-state flux ratio will be independent of the stability of the intermediate states and is only affected by the free energy barriers. For example, consider

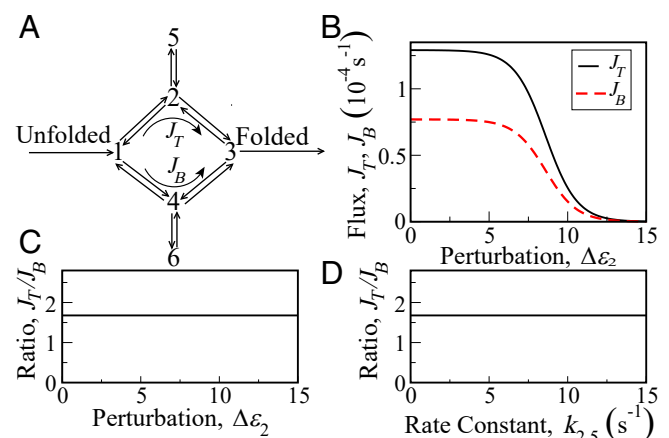


Fig. 2. Steady-state fluxes and their ratio for a protein folding network from folding pathways in hen egg-white lysozyme from refs. 27 and 33. (A) Protein folding network through two independent pathways via intermediate states 2 and 4 (with misfolded error states 5 and 6) to reach the folded conformation in state 3 from the unfolded state 1. (B) Steady-state fluxes J_T and J_B that decay to zero as a function of the energy perturbation $\Delta\epsilon_2$. (C) Ratio of the steady-state fluxes J_T/J_B as a function of the energy perturbation $\Delta\epsilon_2$. (D) J_T/J_B as a function of the rate constant $k_{2,5}$ for the reaction $2 \rightarrow 5$.

a change in the energy of state 2 by $\Delta\epsilon_2$. This perturbation will change both J_T and J_B proportionally in Fig. 2B. As a result, the ratio of the steady-state fluxes J_T/J_B does not change as a function of $\Delta\epsilon_2$ (Fig. 2C). The result is also apparent from the analytic expression for J_T/J_B (SI Appendix, Eq. S28). Notably, the presence of the misfolded error states 5 and 6 is mathematically equivalent to the perturbations of the energy of states 2 and 4, respectively. Therefore, the ratio of the steady-state fluxes J_T/J_B does not depend on the rate constant going into or out of these states (e.g., $k_{2,5}$ in Fig. 2D). Thus, the stability or presence of a misfolded error state does not affect how the steady-state flux splits between the two folding pathways. Notably, identical results can also be obtained using the approach developed in ref. 36. However, our approach is arguably more general as it extends to the networks with futile cycles.

KPR Network. Enzymatic catalysis in the presence of right (cognate) and wrong (noncognate) substrates can often achieve high selectivity through KPR mechanisms with the use of guanosine triphosphate (GTP)/ATP hydrolysis energy. For such networks, the flux distribution can be used to quantify the probability of reaching the wrong product state (error rate) or the probability of futile cycles that result in hydrolysis without any product formation. Here we consider a KPR network that enhances the accuracy of aa-tRNA selection in the *E. coli* ribosome (19, 28, 29, 34) during protein translation, and it is shown in Fig. 3A. It contains two symmetric cycles involving the right R (cognate) or the wrong W (noncognate) aa-tRNA molecules and two ways to reset from states 3/5 to the initial state 1. This can occur via a catalytic step resulting in product formation (rates $k_{3,1}^{(2)}/k_{5,1}^{(2)}$) or via a proofreading step that results in aa-tRNA excision (rates $k_{3,1}^{(1)}/k_{5,1}^{(1)}$). The steady-state ratios of the corresponding fluxes define important system properties of the enzyme.

The error rate can be defined as the fraction of times the noncognate amino acid is incorporated into a protein, that is, as a ratio of $J_W = k_{5,1}^{(2)}P_5 - k_{1,5}^{(2)}P_1$ to $J_R = k_{3,1}^{(2)}P_3 - k_{1,3}^{(2)}P_1$. Per-

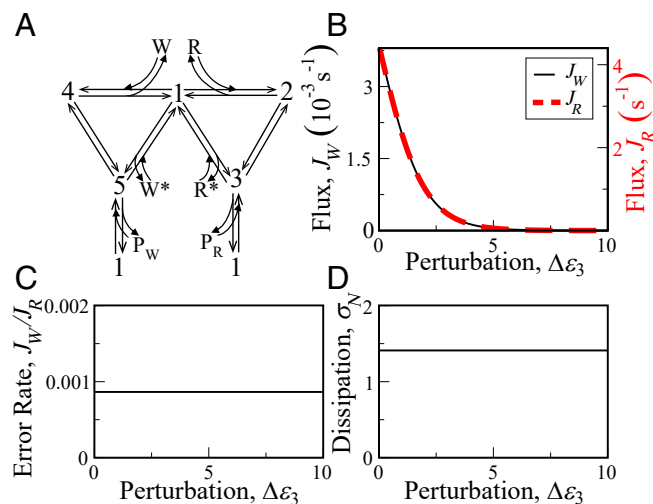


Fig. 3. Steady-state fluxes and their ratios for the KPR network describing aa-tRNA selection in the *E. coli* ribosome. (A) KPR scheme where the right R or the wrong W aa-tRNA molecule can bind to free enzyme state 1. The network from kinetic schemes in refs. 25, 30, 31 comprises two cycles: a proofreading cycle with R^* or W^* and a product formation cycle with products P_R or P_W . (B) Steady-state fluxes for addition of the wrong amino acid J_W and the right amino acid J_R that decay to zero as a function of the energy perturbation $\Delta\epsilon_3$. (C) Error rate J_W/J_R . (D) Normalized energy dissipation σ_N .

turbations of the energy of an intermediate state (e.g., state 3 in Fig. 3 B–D) will change the individual fluxes in Fig. 3B, but the ratio of the fluxes in Fig. 3C will remain invariant. This is a straightforward consequence of Eq. 8, and it generalizes the result of ref. 25. We can also conclude that the error rate will be invariant to perturbations of the discrete-state energies even in the presence of multiple competing pathways, multiple intermediate states, and/or multiple proofreading reactions. Therefore, the error rate in more complex KPR networks is under kinetic control as long as it can be expressed as a ratio of the steady-state fluxes in the linear chemical kinetic framework.

Energy efficiency of the ribosome can be quantified by looking at the number of GTP molecules hydrolyzed per peptide bond (19) or as the energy dissipation per product formed normalized by the GTP hydrolysis energy, that is,

$$\sigma_N \equiv \frac{\sigma}{J_p \Delta\mu_{\text{proof}}} = \frac{J_{\text{proof}}}{J_p} + \frac{\Delta\mu_p}{\Delta\mu_{\text{proof}}}. \quad [9]$$

Here, σ is the total energy dissipation in the nonequilibrium system, while $\Delta\mu_{\text{proof}}$ and $\Delta\mu_p$ are the respective chemical potential differences of the proofreading and the catalytic cycles in the biochemical network. The product formation flux is $J_p = J_R + J_W$, and the proofreading flux is given by $J_{\text{proof}} = k_{3,1}^{(1)}P_3 - k_{1,3}^{(1)}P_1 + k_{5,1}^{(1)}P_5 - k_{1,5}^{(1)}P_1$. The ratio of these fluxes and the normalized energy dissipation σ_N will again be invariant to the energy perturbation of an intermediate state, for example, $\Delta\epsilon_3$ (Fig. 3D).

Myosin-V Network. Motor proteins belong to a broad class of enzymes that convert chemical energy (e.g., from ATP hydrolysis) to perform mechanical work in cells. For example, motor proteins in cells that hydrolyze ATP use the hydrolysis energy to walk on the cytoskeletal track while transporting loads of intracellular cargo (20, 22). The motors are often described by kinetic models (22) that allow one to predict the flux distribution that defines important properties such as the probability of forward or backward steps or probability that the motor proteins hydrolyze ATP but remain at the same position on the track.

Here, for illustration, we examine a kinetic model for myosin-V in Fig. 4A that shows the intermediate states through which the motor protein proceeds as it attempts to move one ~ 36 -nm step along an actin filament (24). The myosin-V network has a main stepping cycle (via states 1 to 5), where the motor protein takes one step forward or backward on the actin filament, and a futile cycle, where the motor protein makes no net movement on the actin filament (via states 2, 3, 4, and 6). During the futile cycle, myosin-V does not move one step along the actin filament, and all of the energy from ATP hydrolysis is wasted. This is not the case for the main stepping cycle, where myosin-V uses the energy available from ATP hydrolysis to take one step forward along the actin filament while doing mechanical work against a load.

The fraction of times that myosin-V takes a backward step is given by the ratio of the backward stepping flux $J_B = k_{2,1}P_2$ to the forward stepping flux $J_F = k_{1,2}P_1$. If the energy of an intermediate state is perturbed, for example, by $\Delta\epsilon_2$, the individual fluxes J_B and J_F in Fig. 4B will change as well. However, the ratio of the backward to forward fluxes in Fig. 4C is invariant to the energy perturbation. This result is easily seen to be a consequence of Eq. 8 for the motion of the myosin-V motor protein. Moreover, we can conclude that this ratio of the backward and forward stepping fluxes will remain invariant regardless of how many intermediate states or futile cycles are present on the mechanochemical network.

The energy efficiency of myosin-V can be defined as the fraction of ATP hydrolysis energy consumed during one step on the

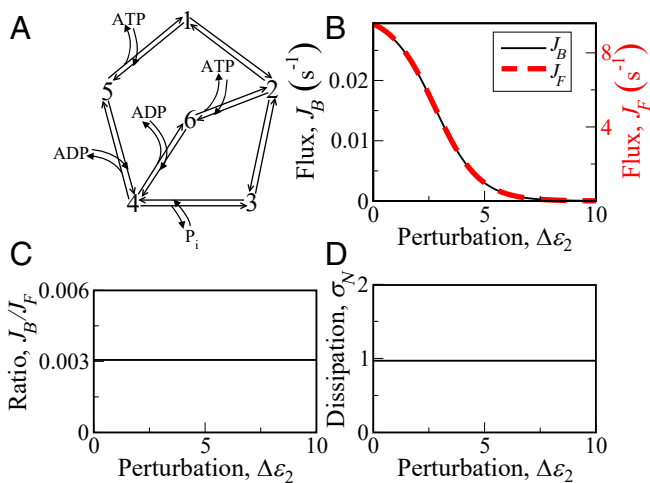


Fig. 4. Steady-state fluxes and their ratios for the mechanochemical network of the two-headed myosin-V motor protein while taking one step on an actin cytoskeleton filament. (A) Mechanochemical network for the myosin-V motor protein from ref. 24 comprising two cycles: a futile cycle and a main stepping cycle. (B) Steady-state fluxes for backward steps J_B and forward steps J_F of myosin-V that decay to zero as a function of the energy perturbation $\Delta\epsilon_2$. (C) Ratio of backward to forward steps J_B/J_F . (D) Normalized energy dissipation σ_N .

track (22) or as the energy dissipation per step normalized by the energy expended from ATP hydrolysis, that is,

$$\sigma_N \equiv \frac{\sigma}{J_{\text{main}} \Delta\mu_{\text{futile}}} = \frac{J_{\text{futile}}}{J_{\text{main}}} + \frac{\Delta\mu_{\text{main}}}{\Delta\mu_{\text{futile}}}. \quad [10]$$

Here, σ is the total energy consumed during the mechanochemical process, and $\Delta\mu_{\text{futile}}$ and $\Delta\mu_{\text{main}}$ are the respective chemical potential differences of the futile cycle and the main stepping cycle. The main stepping flux is $J_{\text{main}} = k_{1,2}P_1 - k_{2,1}P_2$, and the futile flux is $J_{\text{futile}} = k_{6,2}P_6 - k_{2,6}P_2$. The ratio of these two fluxes and the normalized energy dissipation σ_N are also invariant to energy perturbations of an intermediate state such as $\Delta\epsilon_2$ on the mechanochemical cycle (Fig. 4D).

Discussion

Our main theoretical result shows that the ratios of steady-state fluxes are independent of energy perturbations of the intermediate states on biochemical networks that describe a wide class of biological processes. This result can be explained using the following arguments. The energy perturbation at the specific site leads to a change in the stationary probability of the perturbed state and the transition rates out of the perturbed state. However, the effect of the perturbation is opposite for these two properties. If the perturbation increases (decreases) the stationary probability by the exponent of the energy perturbation, it simultaneously decreases (increases) the outgoing transition rates by the same factor. In addition, because the total probability in the system is conserved, the stationary probabilities of all of the states should be modified by the same normalization parameter. This leads to changes in all of the steady-state fluxes in the system by the same parameter, including the fluxes out of the perturbed state where the changes in the stationary probability are compensated by changes in the outgoing transition rates. As a result, all of the steady-state fluxes are scaled in the same way, and their ratios remain constant.

The important implication of our theoretical results is that the properties of major biological processes that depend on the ratios of steady-state fluxes are governed by kinetic rather than thermodynamic (energetic) factors of the underlying free

energy landscapes. Specifically, the ratios of any two steady-state fluxes depend on the transition state energies, but not on the energies of the discrete (internal) states on the free energy landscape. Consequently, the physicochemical properties of biological systems that depend on the ratios of the steady-state fluxes are exclusively under kinetic control, and any changes in the well depths of the individual states do not affect these properties. Therefore, the only way to modify these properties is to change the energy barriers between the intermediate states. Moreover, the invariance result is still valid if several energy perturbations are simultaneously occurring in the system because these perturbations are local, and the total effect of the perturbations is additive. However, the properties of the systems expressed in terms of individual fluxes and/or state probabilities are still affected by perturbations of the discrete-state energies and, therefore, are subject to a combination of thermodynamic and kinetic control.

Our theory is applicable to kinetic models of biochemical systems that, from a single-molecule perspective, are described by linear master equations, that is, they only involve quasi-first-order transitions between the discrete states. Despite this limitation, the framework still applies to a wide range of biological processes under the commonly used assumption of timescale separation (12). These processes include enzyme catalysis and allosteric control, processive motion of molecular motors, receptor signal transduction, ion channel transport, transcriptional regulation, and posttranslational modification (12). To illustrate the biological relevance of our theoretical findings, we applied them to three major biological processes, namely, protein folding via multiple pathways, aa-tRNA selection during protein translation, and the myosin-V molecular motor dynamics. Our examples reveal some counterintuitive implications for specific experimentally observable quantities.

For the protein folding network motivated by the hen egg-white lysozyme system, we find that the splitting fractions for the different pathways along which the protein can fold do not depend on the energy (well depths) of the intermediate states as long as the transition-state energies are constant. Mathematically, such perturbations are equivalent to the introduction of misfolded error states (26, 27). Our invariance results imply that the existence of such states or generally the existence of multistate dead-end branches from the intermediate states will not affect the splitting fractions. The results are clearly generalizable to kinetic models of protein folding in which multiple stable folding conformations are present, for example, when there is a possibility of prion states (37). Our results also imply that the flux splitting between the native and prion conformations would require changes in the free energy barriers and not in the well depths along each of the folding pathways. Thus, a drug that binds to and stabilizes the intermediate but needs to dissociate before the transition states are reached cannot affect the flux splitting.

Our examination of the biochemical network for aa-tRNA selection in the *E. coli* ribosome (19, 23, 25, 30, 31) demonstrates that our invariance statement holds in the presence of energy-dissipating cycles on the network. We show that both the error fraction and the normalized energy dissipation can be expressed as flux ratios, and, therefore, they are invariant to changes in the energies of the intermediate states on the underlying free energy landscape. Hence, genetic mutations in the ribosome (28, 34) that cause changes in these properties must affect the kinetic features of the free energy landscape.

Finally, for the physicochemical properties of myosin-V, we show that the ratio of the forward and backward stepping fluxes and the normalized energy dissipation are invariant to energy perturbations of all of the intermediate states. This indicates that the energy expenditure from ATP hydrolysis during the processive motion of the myosin-V motor protein (20, 22, 24) is

exclusively under kinetic control as long as the external force F_{external} remains constant. Consequently, drugs that specifically stabilize different states on the mechanochemical network for myosin-V but have to dissociate before the transition to the next or to the previous state can occur do not affect the ratio of the energy efficiency or the ratio of the forward to backward steps.

We note that the stationary flux ratios will change if the energy perturbations of individual states are coupled to changes in the free energy barriers. However, our invariance results can have important implications for such cases. Identical effects on the steady-state flux ratios are expected from two mutations stabilizing the transition state by the same mechanism and thus resulting in identical changes of the transition state energy barriers $\epsilon_{i,j}^\ddagger$. That will be the case even if mutations affect the state stabilities ϵ_i differently (see *SI Appendix* for discussion on energy coupling in protein folding from Φ -value analysis). Therefore, even for the perturbations affecting both the energy barriers and the energies

of the states, it is important to know that the changes in the latter do not affect the physical properties that depend on the flux ratios.

Our theoretical study presents a general statement on how kinetic models that provide a quantitative description of a wide class of biological systems can be affected by the underlying features of the free energy landscape. This result pinpoints a hidden symmetry in the underlying equations, which places important constraints on the mechanism for the regulation of important system-level properties. It will be important to see the implication of the invariance results for other biological systems and to determine whether the result can be extended to an asymptotic flux behavior away from the steady state.

ACKNOWLEDGMENTS. This work was supported by Center for Theoretical Biological Physics NSF Grant PHY-1427654. O.A.I. also acknowledges support from Welch Foundation Grant C-1995. A.B.K. also acknowledges support from Welch Foundation Grant C-1559, and from NSF Grants CHE-1664218 and MCB-1941106. We thank Qiwei Yu for useful suggestions.

1. I. H. Segel, *Enzyme Kinetics: Behavior and Analysis of Rapid Equilibrium and Steady State Enzyme Systems* (Wiley, New York, New York, 1975).
2. A. Cornish-Bowden, *Fundamentals of Enzyme Kinetics* (Wiley, 2013).
3. T. Kuhlman, Z. Zhang, M. H. Saier, T. Hwa, Combinatorial transcriptional control of the lactose operon of *Escherichia coli*. *Proc. Natl. Acad. Sci. U.S.A.* **104**, 6043–6048 (2007).
4. H. D. Kim, E. K. O'Shea, A quantitative model of transcription factor-activated gene expression. *Nat. Struct. Mol. Biol.* **15**, 1192–1198 (2008).
5. J. Narula, O. Igoshin, Thermodynamic models of combinatorial gene regulation by distant enhancers. *IET Syst. Biol.* **4**, 393–408 (2010).
6. J. Estrada, F. Wong, A. DePace, J. Gunawardena, Information integration and energy expenditure in gene regulation. *Cell* **166**, 234–244 (2016).
7. K. L. Pierce, R. T. Premont, R. J. Lefkowitz, Seven-transmembrane receptors. *Nat. Rev. Mol. Cell Biol.* **3**, 639–650 (2002).
8. J. P. Changeux, S. J. Edelman, Allosteric mechanisms of signal transduction. *Science* **308**, 1424–1428 (2005).
9. D. Colquhoun, Agonist-activated ion channels. *Br. J. Pharmacol.* **147**, S17–S26 (2006).
10. S. Prabhakaran, G. Lippens, H. Steen, J. Gunawardena, Post-translational modification: nature's escape from genetic imprisonment and the basis for dynamic information encoding. *Wiley Interdiscip. Rev. Syst. Biol. Med.* **4**, 565–583 (2012).
11. J. Gunawardena, Time-scale separation–Michaelis and Menten's old idea, still bearing fruit. *FEBS J.* **281**, 473–488 (2014).
12. J. Gunawardena, A linear framework for time-scale separation in nonlinear biochemical systems. *PLoS One* **7**, e36321 (2012).
13. D. E. Makarov, *Single Molecule Science: Physical Principles and Models* (CRC, 2015).
14. K. J. Laidler, *Chemical Kinetics* (Prentice Hall, 1987).
15. T. L. Hill, *Free Energy Transduction and Biochemical Cycle Kinetics* (Courier Corporation, 2005).
16. G. K. Ackers, A. D. Johnson, M. A. Shea, Quantitative model for gene regulation by lambda phage repressor. *Proc. Natl. Acad. Sci. U.S.A.* **79**, 1129–1133 (1982).
17. L. Bintu *et al.*, Transcriptional regulation by the numbers: Models. *Curr. Opin. Genet. Dev.* **15**, 116–124 (2005).
18. P. Sartori, S. Pigolotti, Kinetic versus energetic discrimination in biological copying. *Phys. Rev. Lett.* **110**, 188101 (2013).
19. J. J. Hopfield, Kinetic proofreading: A new mechanism for reducing errors in biosynthetic processes requiring high specificity. *Proc. Natl. Acad. Sci. U.S.A.* **71**, 4135–4139 (1974).
20. J. Howard, Molecular motors: Structural adaptations to cellular functions. *Nature* **389**, 561–567 (1997).
21. A. Murugan, D. A. Huse, S. Leibler, Discriminatory proofreading regimes in non-equilibrium systems. *Phys. Rev. X* **4**, 021016 (2014).
22. A. B. Kolomeisky, *Motor Proteins and Molecular Motors* (CRC, Boca Raton, FL, 2015).
23. J. Ninio, Kinetic amplification of enzyme discrimination. *Biochimie* **57**, 587–595 (1975).
24. K. I. Skau, R. B. Hoyle, M. S. Turner, A kinetic model describing the processivity of myosin-V. *Biophys. J.* **91**, 2475–2489 (2006).
25. K. Banerjee, A. B. Kolomeisky, O. A. Igoshin, Accuracy of substrate selection by enzymes is controlled by kinetic discrimination. *J. Phys. Chem. Lett.* **8**, 1552–1556 (2017).
26. S. W. Englander, L. Mayne, M. M. Krishna, Protein folding and misfolding: Mechanism and principles. *Q. Rev. Biophys.* **40**, 1–41 (2007).
27. M. M. Krishna, S. W. Englander, A unified mechanism for protein folding: Predetermined pathways with optional errors. *Protein Sci.* **16**, 449–464 (2007).
28. H. S. Zaher, R. Green, Fidelity at the molecular level: Lessons from protein synthesis. *Cell* **136**, 746–762 (2009).
29. N. M. Reynolds, B. A. Lazazzera, M. Ibba, Cellular mechanisms that control mistranslation. *Nat. Rev. Microbiol.* **8**, 849–856 (2010).
30. K. Banerjee, A. B. Kolomeisky, O. A. Igoshin, Elucidating interplay of speed and accuracy in biological error correction. *Proc. Natl. Acad. Sci. U.S.A.* **114**, 5183–5188 (2017).
31. J. D. Mallory, A. B. Kolomeisky, O. A. Igoshin, Trade-offs between error, speed, noise, and energy dissipation in biological processes with proofreading. *J. Phys. Chem. B* **123**, 4718–4725 (2019).
32. T. H. Lowry, K. S. Richardson, *Mechanism and Theory in Organic Chemistry* (Harper & Row, 1987).
33. O. Bieri, G. Wildegger, A. Bachmann, C. Wagner, T. Kiefhaber, A salt-induced kinetic intermediate is on a new parallel pathway of lysozyme folding. *Biochemistry* **38**, 12460–12470 (1999).
34. H. S. Zaher, R. Green, Hyperaccurate and error-prone ribosomes exploit distinct mechanisms during tRNA selection. *Mol. Cell* **39**, 110–120 (2010).
35. C. M. Dobson, Protein folding and misfolding. *Nature* **426**, 884 (2003).
36. A. Berezhkovskii, G. Hummer, A. Szabo, Reactive flux and folding pathways in network models of coarse-grained protein dynamics. *J. Chem. Phys.* **130**, 05B614 (2009).
37. S. B. Prusiner, Prions. *Proc. Natl. Acad. Sci. U.S.A.* **95**, 13363–13383 (1998).